Supplementary Information for:

$BiMnPO_5$ with ferromagnetic Mn^{2+}-(μ-O)$_2$-Mn^{2+} units: a model for magnetic exchange in edge-linked $Mn^{2+}O_6$ octahedra.

Rukang Li,[a,b] Ronald I. Smith[c] and Colin Greaves[d]

[a]Beijing Centre for Crystal Research and Development, Key Laboratory of Functional Crystals and Laser Technology, Technical Institute of Physics and Chemistry, Chinese Academy of Sciences. Beijing 100190, China
[b]Center of Materials Science and Optoelectronics Engineering, University of Chinese Academy of Sciences. Beijing 100049, China.
[c]ISIS facility, RAL, Chilton, Didcot, Oxon OX11 0QX, United Kingdom
[d]School of Chemistry, University of Birmingham, Birmingham B15 2TT, UK

Contents

1. Synthesis and Methods

Samples of $BiMnPO_5$ were prepared by carefully heating a stoichiometric mixture of MnO (previously obtained by reducing MnO_2 in a flowing mixture of 10% H_2 / 90% N_2 at 800 °C for 48 hours), $NH_4H_2PO_4$ and Bi_2O_3 from 300°C to 800°C in air.[1] Since heating above 820°C resulted in decomposition, the target phase was obtained using a final heating at 800°C for a week with intermittent grinding. The phase purity at each stage was monitored with a Siemens D5000 X-ray diffractometer in transmission mode with monochromatic $CuK\alpha_1$ radiation and a position sensitive detector. Time-of-flight NPD data were collected from a 2-3 g sample in a vanadium tube at the instrument POLARIS (earlier design than the current instrument) at ISIS, RAL, Oxford, UK.[2] Data were obtained at ambient temperature and 1.8 K, achieved in an AS Scientific "Orange" cryostat with continuous pumping. Rietveld structure refinements on the collected XRD and NPD patterns were carried out using GSAS[3] with the EXPGUI interface.[4] The magnetic order was initially determined using the nuclear unit cell (space group $P2_1/n$), appropriately enlarged to allow for the additional magnetic reflections. Subsequently, this was converted to the standard setting of $P2_1/c$ for the magnetic cell (giving the magnetic space group P_a2_1/c) but $P2_1/n$ was retained for the nuclear structure to allow direct comparison with litersture reports. No individual magnetic reflections were apparent for $Mn_3P_2O_8$ in the range from 4-12Å (see Fig. 2a in the main text and Fig. S1). Any magnetic contribution at lower d values would be insignificant so the magnetic contribution was ignored.

Ab initio calculations on a model of $Mn_2O_2(H_2O)_8$ with experimental geometry and variable Mn–Mn distances were performed using the CRYSAL17 code;[5] a recently developed triple-zeta variable polarization (TZVP) basis set was applied to all the atoms in the molecule.[6] The calculation was done on a DFT level with a hybrid functional (α = 0.10) of B3LYP parameterization.[7,8] The total energies of the model with FM and AFM coupling of the two Mn(II) ions were obtained and the Heisenberg exchange parameters (J) were deduced with the expression proposed by Yamaguchi *et al*:[9]

$$J = \frac{E^{LS} - E^{HS}}{< S^2 >^{HS} - < S^2 >^{LS}} \qquad (1)$$

2. Figures

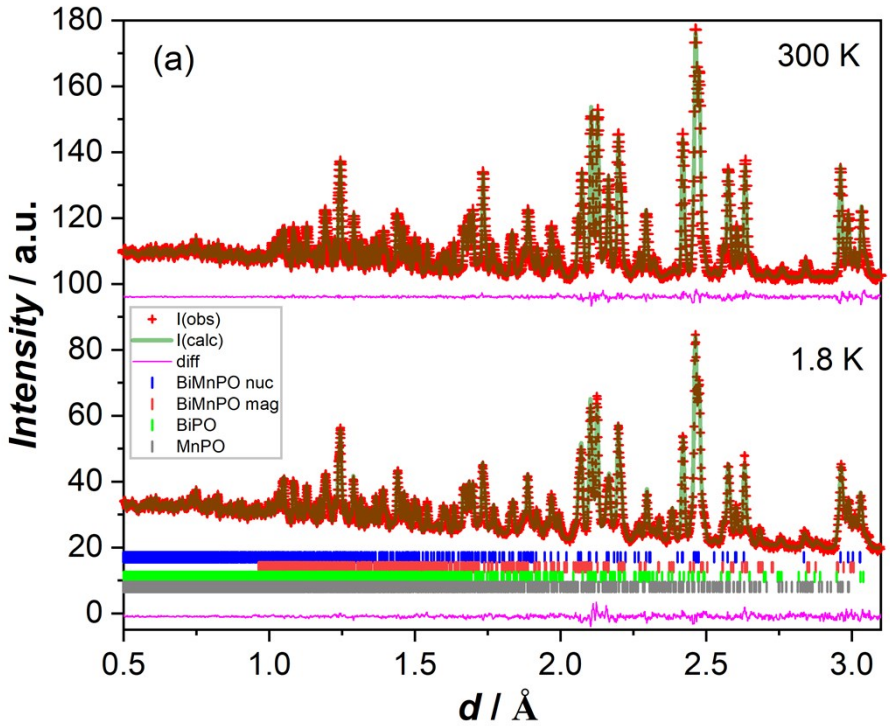

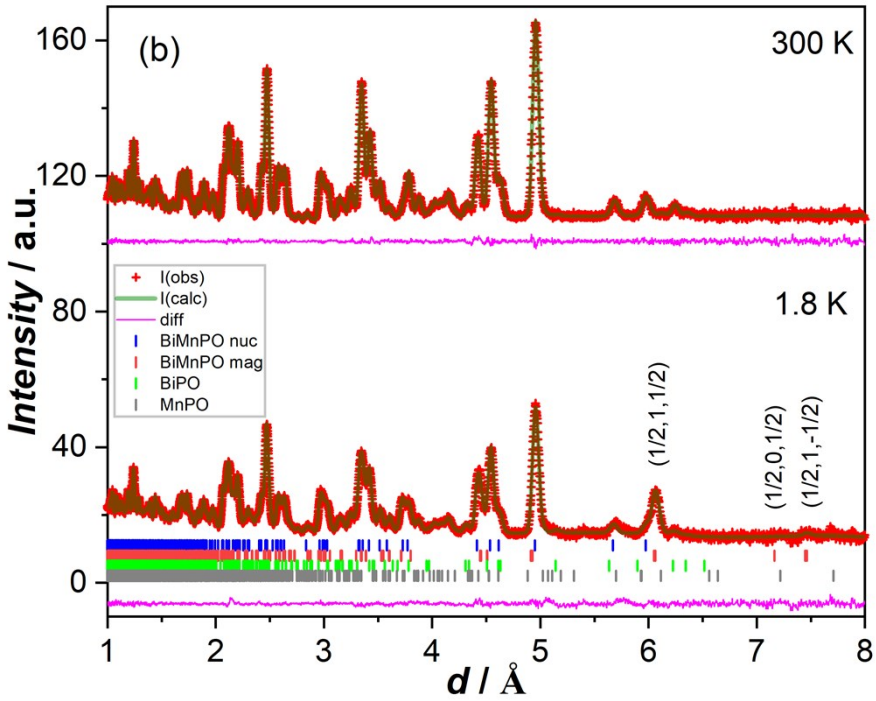

Figure S1 Rietveld refinement plots at 300 K and 2 K for (a) the 145° detector and (b) the 35° detector. The 300 K data are offset by ~90 units.

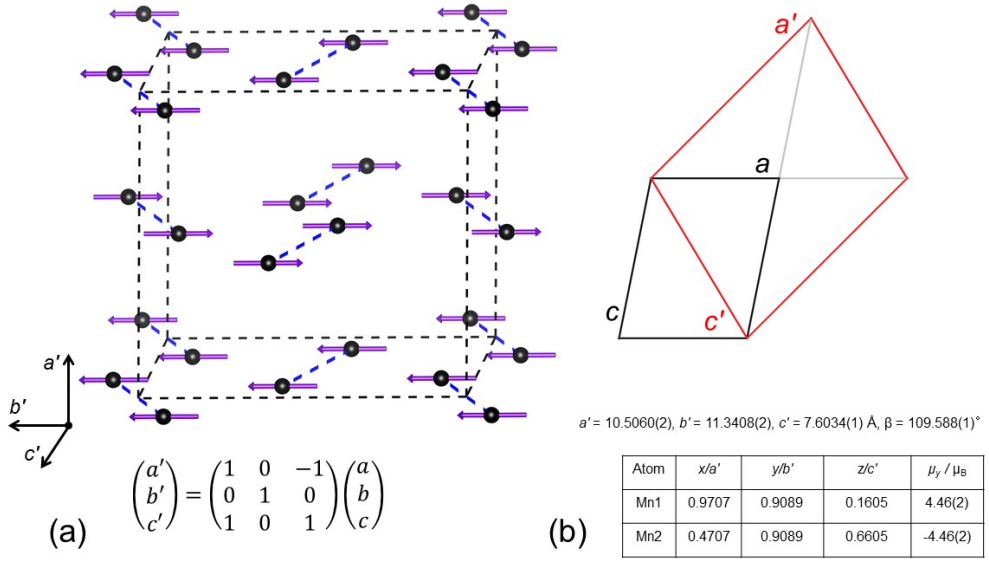

Atom	x/a'	y/b'	z/c'	μ_y / μ_B
Mn1	0.9707	0.9089	0.1605	4.46(2)
Mn2	0.4707	0.9089	0.6605	-4.46(2)

Figure S2 (a) The magnetic unit cell (a',b',c') showing the magnetic order in $BiMnPO_5$ (only Mn, black spheres, shown) and the full transformation matrix; (b) the transformation of the unit cell perpendicular to the *b*-axis, the new unit cell and magnetic data for the unit cell.

90° Direct and 180° Superexchange

GKA mechanism, Very Strong AFM

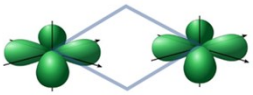

I: $d_{xy} - d_{xy}$

$$J_{dd} \sim -\frac{t_{dd}^2}{U_{dd}}$$

$-24.20\ meV$

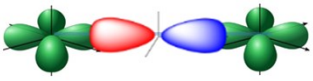

II: $d_{x^2-y^2} - P_x - d_{x^2-y^2}$

$$J_S^{\sigma} \sim -\frac{t_{pd\sigma}^4}{\Delta^2}\left(\frac{1}{U_{dd}} + \frac{1}{2\Delta + U_{pp}}\right)$$

$-25.31\ meV$

Strict Orthogonality

O. Kahn mechanism, Strong FM

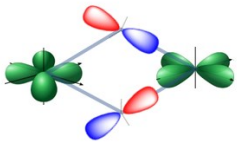

III: $d_{xy} - P_y - d_{x^2-y^2} - P_x - d_{xy}$

$$J_K^{\sigma\pi} \sim \frac{t_{pd\sigma}^2 t_{pd\pi}^2}{\Delta^2}\left(\frac{1}{U_{dd}} + \frac{1}{2\Delta + U_{pp}}\right)$$

$7.20\ meV$

GKA mechanism, moderate AFM

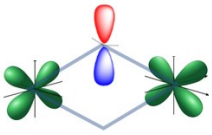

IV: $d_{yz} - P_z - d_{xz}$

$$J_S^{\pi} \sim -\frac{t_{pd\pi}^4}{\Delta^2}\left(\frac{1}{U_{dd}} + \frac{1}{2\Delta + U_{pp}}\right)$$

$-2.05\ meV$

Accidental Orthogonality

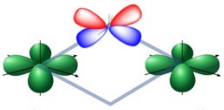

$d_{xy} - P_x \perp P_y - d_{xy}$

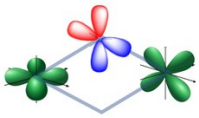

$d_{xy} - P_x \perp P_z - d_{xz}$

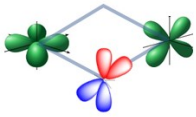

V: $d_{xy} - P_y \perp P_z - d_{yz}$

$$J_{AO}^{\pi} \sim \frac{t_{pd\pi}^4 J_H^P}{\Delta^2 (2\Delta + U_{pp})^2}$$

$0.11\ meV$

GKA mechanism, moderate AFM

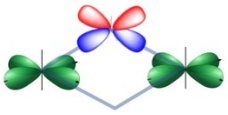

VI: $d_{x^2-y^2} - P_x \perp P_y - d_{x^2-y^2}$

$$J_{AO}^{\sigma} \sim\sim \frac{t_{pd\sigma}^4 J_H^P}{\Delta^2 (2\Delta + U_{pp})^2}$$

$1.37\ meV$

Figure S3 Magnetic exchange pathways in Di-manganese (II, II) pairs with edge-shared Mn-(μ-O)2-Mn bonds. Green, Mn3*d*-orbitals; red/blue O2*p* showing phase.

3. References

1. X. Xun, S. Uma and A.W. Sleight, *J. Alloys and Compounds* 2002, **338**, 51-53.
2. R. I. Smith, S. Hull and A. R. Armstrong, "The Polaris Powder Diffractometer at ISIS.", in Proceedings of the 3rd European Powder Diffraction Conference, Vienna, Austria, 1993, (Ed. R. Delhez and E.J. Mittemeijer), *Mater. Sci. Forum* 1994, **166-169**, 251-256.
3. A. C. Larson and R. B. Von Dreele, "General Structure Analysis System (GSAS)," 2000.
4. B. H. Toby, EXPGUI, a graphical user interface for GSAS, *J. Appl. Crystallogr*. 2001, **34**, 210–213.
5. R. Dovesi, F. Pascale, B. Civalleri, K. Doll, N. M. Harrison, I. Bush, P. DArco, Y. Noel, M. Rerat, P. Carbonniere, M. Causa, S. Salustro, V. Lacivita, B. Kirtman, A. M. Ferrari, F. S. Gentile, J. Baima, M. Ferrero, R. Demichelis and M. D. La Pierre, *J. Chem. Phys.* 2020, **152**, 204111.
6. M. F. Peintinger, D. Vilela Oliveira and T. Bredow, *J. Comput. Chem.* 2013, **34,** 451-459.
7. A. D. Becke, *J. Chem. Phys*. 1993, **98**, 5648-5652.
8. P. J. Stephens, F. J. Devlin, C. F. Chabalowski and M. J. Frisch, *J. Phys. Chem.* 1994, **98**, 11623–11627.
9. K. Yamaguchi, H. Fukui and T. Fueno, *Chem. Lett.* 1986, **15**, 625–628.